

Signatures of the Pair-Coherent State

A. Gilchrist* and W.J. Munro†

* School of Computing and Mathematical Sciences, University of Waikato, Hamilton, New Zealand

† Centre for Laser Science, Department of Physics, University of Queensland,

QLD 4072, Brisbane, Australia

(November 12, 2018)

We explore in detail the possibility of generating a pair-coherent state in the non-degenerate parametric oscillator when decoherence is included. Such states are predicted in the transient regime in parametric oscillation where the pump mode is adiabatically eliminated. Two specific signatures are examined to indicate whether the state of interest has been generated, the Schrödinger cat state—like signatures, and the fidelity. Solutions in a transient regime reveal interference fringes which are indicative of the formation of a Schrödinger cat state. The fidelity indicates the purity of our prepared state compared to the ideal pair-coherent state.

I. INTRODUCTION

Quantum mechanics is well known for two fundamental quantities, the superposition of states and entanglement. Both have been studied extensively and much rich physics has been observed. Generally however systems exhibit one but not generally both of these phenomena. Recently however the idealised state produced in non-degenerate parametric oscillation when the pump mode is adiabatically eliminated has been shown to give the possibility of observing both Schrödinger cat states [1] and producing correlated photon pairs which could be used to perform tests of quantum mechanics versus local realism such as the EPR paradox [2] and the Bell inequality [3,4].

There is still much interest in the possibility of generating experimentally a Schrödinger cat state. Such a state is defined as a quantum superposition of two macroscopically distinct states [5]. It was Schrödinger’s concern that quantum mechanics does not fundamentally prohibit the existence of such states, which seemingly defy physical reality. Work by Krippner and Reid [1] predicts that a Schrödinger cat state may be produced in the signal field of non-degenerate parametric oscillation, in a transient regime. The theoretical model presented here incorporates the effect of linear signal losses, which tend to oppose the formation of the superposition state.

Recent work by Gilchrist *et. al.* [3,4] and Munro [6] showed how in a certain narrow regime, the pair-coherent state gives quantum mechanical predictions that are in disagreement with those of local hidden variable theories for a situation involving continuous quadrature phase amplitude measurements. This test could be achieved by binning the continuous position and momentum information into two categories and using the binary results in the strong Clauser Horne Bell inequality test [7]. The predicted violation was small (less than 2%). Such results were highly idealised, and assumed the preparation of a pair-coherent state to begin with.

In this paper we will investigate the possibility of gen-

erating a pair-coherent state in the non-degenerate parametric oscillator with an adiabatically eliminated pump mode when decoherence is included. Two specific signatures of the state will be considered, interference fringes which are indicative of the formation of a Schrödinger cat state and the fidelity. In particular the fidelity will provide an indication of the parameter regime required to perform a loophole free test of quantum mechanics.

It should be noted that the fidelity is a rather abstract quantity and in practice would require the entire state to be reconstructed in order to be measured. The Schrödinger cat state signatures however are more operationally accessible though given the sensitivity of Schrödinger cat state itself to decoherence [8] we would expect similar sensitivity for the pair-coherent state and this is indeed the case.

II. THE PAIR-COHERENT STATE

The following two-mode entangled quantum superposition state,

$$|\text{circle}\rangle_m = \mathcal{N} \int_0^{2\pi} e^{-im\varsigma} |r_0 e^{i\varsigma}\rangle_a |r_0 e^{-i\varsigma}\rangle_b d\varsigma \quad (1)$$

is known as the pair-coherent (or “circle”) state and was originally discussed by Agarwal [9,10] and Reid and Krippner [1]. In equation (1) $|\dots\rangle_a$ and $|\dots\rangle_b$ represent coherent states in the modes \hat{a} and \hat{b} , where the \hat{a} and \hat{b} are the usual boson operators. \mathcal{N} is a normalisation coefficient and r_0 the amplitude of the coherent state. m is the photon number difference between the signal and idler modes. This state is actually a continuous superposition of coherent states in a circle (hence the notation $|\text{circle}\rangle$). For our purposes in this paper we shall concentrate on the $m = 0$ (equal photon number in each mode) situation in equation (1) which when normalised is given by

$$|\text{circle}\rangle = \mathcal{B}^{1/2} \int_0^{2\pi} d\zeta |r_0 e^{i\zeta}\rangle_a |r_0 e^{-i\zeta}\rangle_b, \quad (2)$$

where

$$\mathcal{B}^{-1} = 4\pi^2 e^{-2r_0^2} I_0(2r_0^2), \quad (3)$$

Here I_0 is a zeroth order modified Bessel function. Such a state can also be written in terms of correlated photon number pairs of the form

$$|\Psi\rangle = \sum_{n=0}^{\infty} c_n |n\rangle |n\rangle \quad (4)$$

where

$$c_n = \frac{r_0^{2n}}{n! I_0(2r_0^2)}. \quad (5)$$

Such a state should not be confused with the state produced by the non-degenerate parametric amplifier (NDPA) which can also be written in the form of (4) but now with the c_n coefficients given by

$$c_n = \frac{\tanh^n [\chi\epsilon\tau]}{\cosh [\chi\epsilon\tau]} \quad (6)$$

Here ϵ represents the field amplitude of a non-depleting classical pump, χ is proportional to the susceptibility of the medium and τ is the time that the modes spend in the crystal.

In this paper we are interested in exploring the generation of the pair-coherent state.

III. THE NON-DEGENERATE PARAMETRIC OSCILLATOR

It has been suggested by Reid and Krippner that the NDPO transiently generates a state of the above form, in the limit of very large parametric nonlinearity and high- Q cavities [1]. The non-degenerate parametric oscillator with linear damping in the signal and idler modes and the pump mode pumped by a classical field may be represented by the Hamiltonian

$$\begin{aligned} H &= H_I + H_p + H_{\text{irrev}} \quad (7) \\ H_I &= i\hbar\kappa(a_3 a_2^\dagger a_1^\dagger - a_3^\dagger a_2 a_1) \\ H_p &= i\hbar\epsilon(a_3^\dagger - a_3) \\ H_{\text{irrev}} &= \sum_{jl} (a_j \Gamma_{jl}^\dagger + a_j^\dagger \Gamma_{jl}). \end{aligned}$$

Here a_i are boson operators for the cavity modes at frequencies ω_i , where $\omega_3 = \omega_1 + \omega_2$. The mode a_3 is driven by a resonant external driving field with amplitude proportional to ϵ and is known as the pump-mode. Modes a_1 and a_2 are the signal- and idler-modes. The loss of photons through the cavity mirrors is modeled by the Hamiltonian term H_{irrev} , which denotes a coupling of the cavity

modes to the zero temperature reservoir modes (symbolised by Γ_i) external to the cavity. We will denote the cavity decay rates for the modes a_i by γ_i .

Following standard techniques it is easy to derive a master equation of the form

$$\begin{aligned} \dot{\rho} &= \frac{1}{i\hbar} [H_I + H_p, \rho] \\ &+ \sum_{j=1}^3 \gamma_j (2a_j^\dagger \rho a_j - a_j^\dagger a_j \rho - \rho a_j^\dagger a_j) \quad (8) \end{aligned}$$

In the limit where the pump mode is heavily damped compared to the other modes ($\gamma_3 \gg \gamma_2, \gamma_1$) the pump variables can be eliminated. This is equivalent to studying the following model Hamiltonian:

$$\begin{aligned} H &= i\hbar \frac{\epsilon\kappa}{\gamma_3} (a_2^\dagger a_1^\dagger - a_2 a_1) \\ &- \frac{\kappa^2}{\gamma_3} \sum_l (a_2 a_1 \Gamma_l^\dagger + a_2^\dagger a_1^\dagger \Gamma_l) \\ &+ \sum_{jl} (a_j \Gamma_{jl}^\dagger + a_j^\dagger \Gamma_{jl}). \quad (9) \end{aligned}$$

The presence of the two-photon damping term is the fundamental difference between the NDPO in this limit and the NDPA.

To aid our discussion of parameters below, we will briefly examine realistic parameter values for the non-degenerate parametric oscillator containing the commonly used crystals, silver gallium selenide (AgGaSe₂) and potassium titanyl phosphate (KTP). In Table (I) are shown some typical values. We easily observe that the nonlinear coupling constant is much weaker than the damping constant and hence our scaled parameter $g^2 = \kappa^2/\gamma\gamma_3$ that we will introduce shortly will be very small.

CRYSTAL	$\kappa(s^{-1})$	$\gamma(s^{-1})$	κ/γ
AgGaSe ₂	4.4×10^4	7.5×10^8	5.9×10^{-5}
KTP	7.6×10^3	7.5×10^8	1×10^{-5}

TABLE I. Table of realistic values for the nonlinear coupling constant κ and the damping constant γ for two types of parametric crystal AgGaSe₂ and *KTP*.

IV. THE ADIABATICALLY ELIMINATED MASTER EQUATION

The Hamiltonian (9) above corresponds to the following master equation (equation (8) with the pump mode adiabatically eliminated)

$$\begin{aligned} \frac{d\rho}{d\tau} = & \lambda[a_2^\dagger a_1^\dagger - a_2 a_1, \rho] \\ & -g^2(2a_1^\dagger a_2^\dagger \rho a_1 a_2 - a_1^\dagger a_2^\dagger a_1 a_2 \rho - \rho a_1^\dagger a_2^\dagger a_1 a_2) \\ & + \sum_{j=1}^2 (2a_j^\dagger \rho a_j - a_j^\dagger a_j \rho - \rho a_j^\dagger a_j) \end{aligned} \quad (10)$$

where we have introduced the following scaled variables $\lambda = \frac{\epsilon\kappa}{\gamma_3\gamma}$ and $g^2 = \frac{\kappa^2}{\gamma_3\gamma}$. The time has been scaled such that $\tau = \gamma t$ and we have assumed that the signal and idler decay constant γ_1 and γ_2 are in fact equal to γ .

The master equation can be solved numerically by projecting the master equation onto an infinite number state basis [11]. Expanding the density matrix in the number state basis as follows

$$\rho_{n_1 n_2; m_1 m_2} = \langle n_1 | \langle n_2 | \rho | m_1 \rangle | m_2 \rangle, \quad (11)$$

we may express the time evolution of the system as

$$\begin{aligned} \frac{\partial}{\partial \tau} \rho_{i_1 i_2; j_1 j_2} &= \langle i_1 | \langle i_2 | \frac{\partial}{\partial \tau} \rho | j_1 \rangle | j_2 \rangle \\ &= \mathcal{L}_{i_1 i_2; j_1 j_2}^{n_1 n_2; m_1 m_2} \rho_{n_1 n_2; m_1 m_2} \end{aligned} \quad (12)$$

where this super matrix $\mathcal{L}_{i_1 i_2; j_1 j_2}^{n_1 n_2; m_1 m_2}$ is given by

$$\begin{aligned} \mathcal{L}_{i_1 i_2; j_1 j_2}^{n_1 n_2; m_1 m_2} = & \lambda \sqrt{i_1 i_2} \delta_{i_1, j_1}^{n_1+1, m_1} \delta_{i_2, j_2}^{n_2+1, m_2} \\ & - \lambda \sqrt{(i_1+1)(i_2+1)} \delta_{i_1, j_1}^{n_1-1, m_1} \delta_{i_2, j_2}^{n_2-1, m_2} \\ & + \lambda \sqrt{j_1 j_2} \delta_{i_1, j_1}^{n_1, m_1+1} \delta_{i_2, j_2}^{n_2, m_2+1} \\ & - \lambda \sqrt{(j_1+1)(j_2+1)} \delta_{i_1, j_1}^{n_1, m_1-1} \delta_{i_2, j_2}^{n_2, m_2-1} \\ & - 2g^2 \prod_{k=1}^2 \sqrt{(i_k+1)(j_k+1)} \delta_{i_1, j_1}^{n_1-1, m_1-1} \delta_{i_2, j_2}^{n_2-1, m_2-1} \\ & + g^2 [i_1 i_2 + j_1 j_2] \delta_{i_1, j_1}^{n_1, m_1} \delta_{i_2, j_2}^{n_2, m_2} \\ & + 2\sqrt{(i_1+1)(j_1+1)} \delta_{i_1, j_1}^{n_1-1, m_1-1} \delta_{i_2, j_2}^{n_2, m_2} \\ & - [i_1 + j_1] \delta_{i_1, j_1}^{n_1, m_1} \delta_{i_2, j_2}^{n_2, m_2} \\ & + 2\sqrt{(i_2+1)(j_2+1)} \delta_{i_1, j_1}^{n_1, m_1} \delta_{i_2, j_2}^{n_2-1, m_2-1} \\ & - [i_2 + j_2] \delta_{i_1, j_1}^{n_1, m_1} \delta_{i_2, j_2}^{n_2, m_2} \end{aligned} \quad (13)$$

Here

$$\delta_{i,j}^{n,m} = \begin{cases} 1 & \text{if } i = n \text{ and } j = m \\ 0 & \text{otherwise} \end{cases} \quad (14)$$

To allow for numerical calculations, one must put a finite limit on the number of Fock states used in the basis in (12). Care must be taken to ensure that the truncation of the number state basis is done correctly so the population of the higher order states is small. In practice we found $n_{\max} = 20$ sufficient for most of the calculations.

V. ENTANGLEMENT

As we mentioned in the introduction, this pair-coherent state has the property that it contains sufficient entanglement to violate a Bell inequality. Gilchrist *et al.* showed that the pair-coherent state specified by (1) theoretically violated a Bell inequality. To be more explicit, they showed how using highly efficient quadrature phase homodyne measurements, the Clauser Horne strong Bell inequality could be tested in an all optical regime. While the violation may be small the highly efficient detection means that provided the extremely ideal state could be generated, a significant test could be done.

There are a number of measures to determine the purity of the produced state. The measure we will use here is the fidelity. The fidelity may be defined as

$$F = |\langle \text{circle} | \text{output} \rangle|^2 \quad (15)$$

in terms of pure states. In terms of the density operator $\hat{\rho}$ of the output state, we represent the fidelity as

$$F = \text{Tr} \left[\rho_{\text{circle}}^{1/2} \rho_{\text{output}} \rho_{\text{circle}}^{1/2} \right]^{1/2} \quad (16)$$

Figure 1 shows the result of calculating the fidelity against an ideal pair-coherent state for $\lambda/g^2 = 1.12$ and two different values of g . It shows a maximum fidelity of around 80% for $g^2 = 300$. For larger g we can get a larger fidelity but the transient period over which this is available is significantly shorter. Given the small size of the Bell inequality violation, and the narrow parameter regime over which it occurs in reference [3] it is likely that higher nonlinearities would be required for the NDPO to produce the state sufficient to violate the Bell inequality in that scheme.

Gilchrist: Figure 1

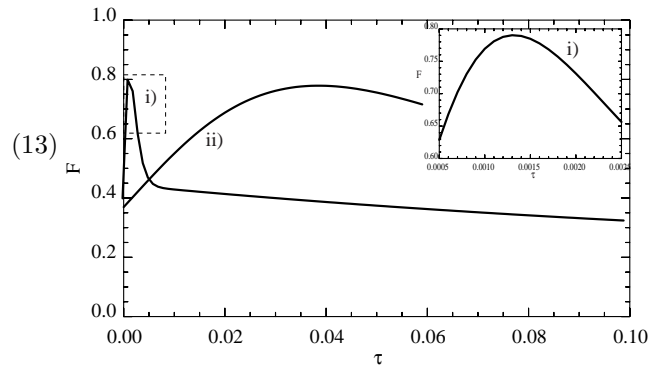


FIG. 1. Plot of the fidelity of the generated state compared with the pair-coherent state for $\lambda/g^2 = 1.12$ and (i) $g^2 = 300$ giving a maximum of $F \sim 0.78$, (ii) $g^2 = 10$ giving a maximum of $F \sim 0.76$.

VI. SCHRÖDINGER CAT STATES

Given a pair-coherent state, previous work by Krippner and Reid [1] has predicted that in the limit of very large r_0 and with a conditional measurement of one mode, a Schrödinger cat state may be produced in the other mode. Observing these states then constitutes an indirect signature of the presence of a pair-coherent state as well as being of interest in its own right. In this section we examine the formation of these states when the parameters are not so extreme and with the presence of damping.

Let us now suppose that one measures the quadrature phase amplitude defined by

$$X_{\theta_i} = (a_i e^{-i\theta_i} + a_i^\dagger e^{i\theta_i}) / \sqrt{2} \quad (17)$$

where θ_i is the phase of the local oscillator for the i th mode. The two measured quadratures X_0 and $X_{\pi/2}$ are non commuting observables. We assume that the measurement of the quadrature X_{θ_i} gives the result x_{θ_i} .

It is then possible to construct the joint probability distribution of obtaining a result x_{θ_1} for the first mode and x_{θ_2} for the second. This probability is expressed as

$$P_{\theta_1, \theta_2}(x_1, x_2) = \langle x_1 | \langle x_2 | \rho | x_2 \rangle | x_1 \rangle \quad (18)$$

Here we have abbreviated x_{θ_1} by x_1 and x_{θ_2} by x_2 . Our state of interest can then be detected by observing interference fringes in the probability distribution $P_{\pi/2, 0}(x_1 = z, x_2 = 0)$ for the quadrature phase amplitude measurement performed on the signal mode, conditioned on the idler mode result $x_2 = 0$ for $\theta_2 = 0$. The observation of interference fringes present in one of the quadrature measurements (in conjunction with the observation of twin isolated peaks in the conjugate quadrature measurement) are indicative of Schrödinger cat states, where X_0 is analogous to the rôle of position and $X_{\pi/2}$ of momentum.

In terms of our number state basis expansion for the density matrix, this joint probability distribution can be written as

$$P_{\theta_1, \theta_2}(x_1, x_2) = \sum_{\substack{n_1, n_2 \\ m_1, m_2=0}}^{\infty} \rho_{n_1 n_2; m_1 m_2} \prod_{i=1}^2 \langle x_{\theta_i} | n \rangle \langle m | x_{\theta_i} \rangle \quad (19)$$

where $\langle x_{\theta_i} | n \rangle$ is given by

$$\langle x_{\theta} | n \rangle = \frac{e^{-in\theta}}{\sqrt{2^n n! \sqrt{\pi}}} \exp\left[-\frac{1}{2}x_{\theta}^2\right] H_n(x_{\theta}) \quad (20)$$

where the units have been chosen such that $\hbar = \omega = c = 1$ and $H_n(x_{\theta})$ is the Hermite polynomial.

A. The ideal situation

In the absence of damping the ideal pair-coherent state is given by (4) with the c_n coefficients specified by (5).

In figure 2 we plot $P_{0,0}(x_1 = z, x_2 = 0)$ versus z and $P_{\pi/2,0}(x_1 = p, x_2 = 0)$ versus p . We clearly observe the interference fringes and twin peaks that characterise the Schrödinger cat state $|i\lambda/g^2\rangle + |-i\lambda/g^2\rangle$.

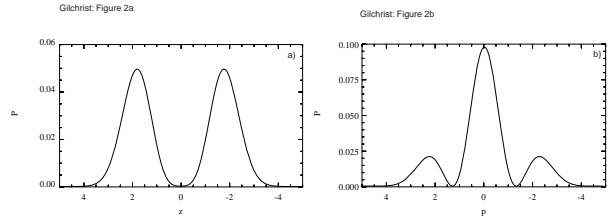


FIG. 2. Plot of position (X_0) (a) and momentum ($X_{\pi/2}$) (b) probability distribution for the signal mode conditioned on a quadrature position measurement on the idler mode recording 0. Here we have $\lambda/g^2 = 1.5$.

For comparison, the Schrödinger cat state signatures are also shown for the pair-coherent state required by Gilchrist *et. al.* ($\lambda/g^2 = 1.12$). As can be expected we do not get very distinct interference fringes and peak-resolution. Interestingly, clear cat signatures require only slightly larger values of λ/g^2 .

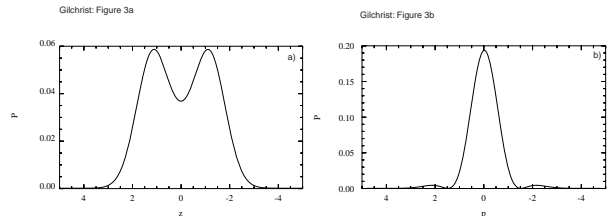


FIG. 3. Plot of position (X_0) (a) and momentum ($X_{\pi/2}$) (b) probability distribution for the signal mode conditioned on a quadrature position measurement on the idler mode recording 0. Here we have $\lambda/g^2 = 1.12$.

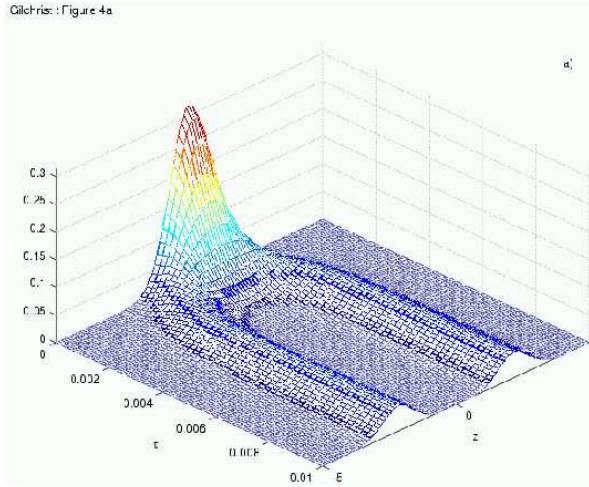
B. Numerical Simulations

The probability distribution is then written as

$$P_{\theta_1, \theta_2}(x_1, x_2) = \sum_{\substack{n_1, n_2 \\ m_1, m_2=0}}^{n_{\max}} \rho_{n_1 n_2; m_1 m_2} \prod_{i=1}^2 \langle x_{\theta_i} | n \rangle \langle m | x_{\theta_i} \rangle \quad (21)$$

In our calculations the effect on increasing the number of basis states by one produced an error of less than 0.001 percent.

The results of our calculations are shown in the Figures 4-5. Figure 4 plots the position (X_0) and momentum ($X_{\pi/2}$) probability distributions versus time. The interference fringes in the momentum probability distribution combined with the twin peaks in the position distribution reveal the Schrödinger cat state-like nature.



Gilchrist: Figure 4a

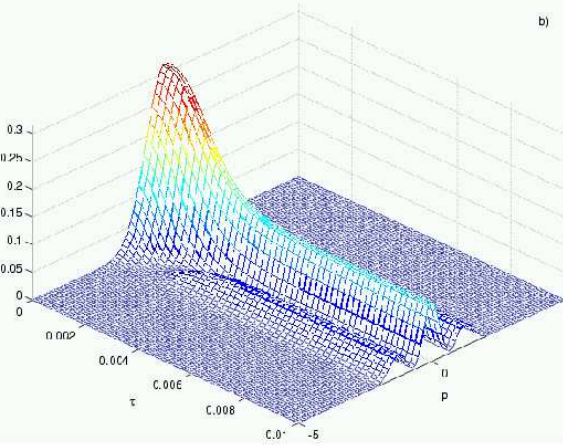
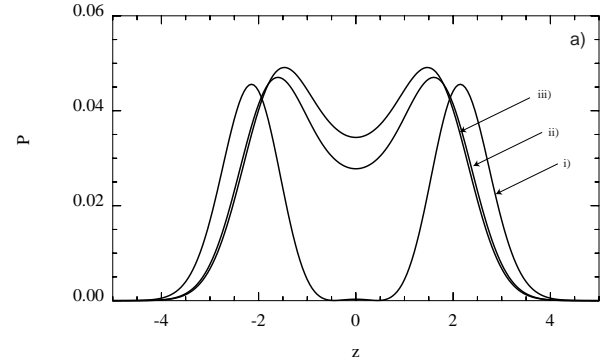


FIG. 4. Plot of (a) the evolution of the position probability distribution $P(z)$, and (b) the momentum probability distribution $P(p)$. Here $g^2 = 300$ with $\lambda/g^2 = 1.5$.

The formation of fringes with the evolution of the signal field from the vacuum state is clearly evident in Figure 4. As the oscillator evolves further the fringes are washed out. The $|i\lambda/g^2\rangle - |-i\lambda/g^2\rangle$ state, which is generated from $|i\lambda/g^2\rangle + |-i\lambda/g^2\rangle$ with the loss of a cavity photon, contributes more significantly as time increases, and the fringes are lost in this case after only 0.1τ .

In order to establish the orders of g required to obtain a clear fringe pattern, the $P(z)$ and $P(p)$ distributions are shown in figure 5 for a range of g with $\lambda/g^2 = 1.5$. For g^2 greater than or of the order of 10, interference fringes become apparent in the transient evolution of the oscillator. The fringes (for fixed λ/g^2) become more pronounced as g increases. This is consistent with the earlier analytical conclusions, which were based on calculations performed in the large g limit where the strength of the two-photon nonlinearity is much greater than the single-photon cavity loss rate.

Gilchrist: Figure 5a



Gilchrist: Figure 5b

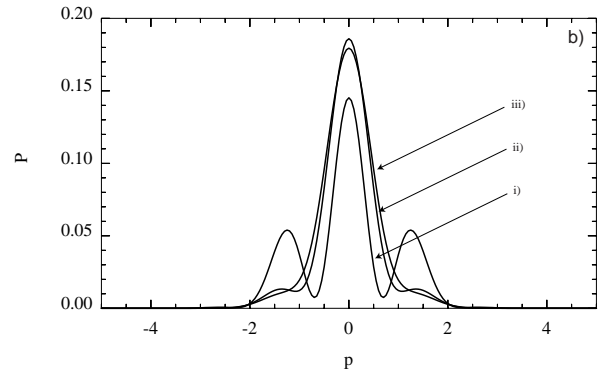


FIG. 5. Plot of (a) the position probability distribution $P(z)$ and (b) the momentum probability distribution $P(p)$; for (i) $g^2 = 300$ with $t = 0.014\tau$, (ii) $g^2 = 10$ with $t = 0.059\tau$, (iii) $g^2 = 3$ with $t = 0.19\tau$. Here $\lambda/g^2 = 1.5$, and the time chosen was informally optimised.

As a final appraisal, we can test the fidelity of the cat state against an ideal Schrödinger cat state of the form $|i\lambda/g^2\rangle + |-i\lambda/g^2\rangle$ and this is shown in figure 6 for various times. Note that it is perfectly possible to generate a Schrödinger cat state not of this form but which still constitutes a superposition of two macroscopically distinct states, hence the fidelity in this case is an indication of the purity of the underlying pair-coherent state rather than an indication of a good Schrödinger cat state.

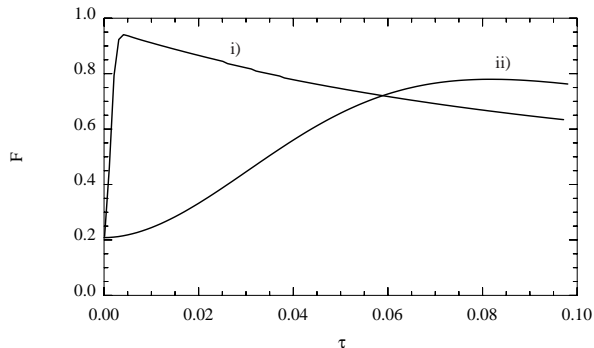


FIG. 6. Plot of the fidelity of the generated cat state for (i) $g^2 = 300$ giving a maximum of $F \sim 0.94$ and (ii) $g^2 = 10$ giving a maximum of $F \sim 0.78$. Here $\lambda/g^2 = 1.5$. The result is conditioned on a quadrature position measurement on the idler mode recording 0

In this section we have established how the non degenerate parametric oscillator operating in an adiabatically eliminated pump mode regime will produce Schrödinger cat states in the transient evolution.

VII. CONCLUSIONS

In this paper we have examined two signatures of the formation of pair coherent states in the NDPO in the presence of linear damping. The most direct indication is to look at the fidelity and even with large nonlinearities we found the fidelity to be poor although higher nonlinearity improves the fidelity. Certainly the acquired fidelity would indicate that the generated state would be a poor candidate for the Bell inequality test of Gilchrist *et al.* even for nonlinearities as high as given by $g^2 \sim 300$.

A more indirect measurement of the purity of the state is to look for the formation of Schrödinger cat states which are predicted upon a conditioned measurement on one mode given a large value for λ/g^2 . The formation of these states not only gives an indication of the presence of a pair-coherent state but are of interest in their own right. Here we predict that for nonlinearities characterised by $g^2 \sim 300$ formation of clear Schrödinger cat states is possible for only $\lambda/g^2 \sim 1.5$. Though, again, this parameter regime is difficult to produce experimentally.

VIII. ACKNOWLEDGEMENTS

WJM and AG both would like to acknowledge the support of the Australian Research Council.

-
- [1] M. Reid and L. Krippner, Phys. Rev. A **47**, 552 (1993).
 - [2] K. Tara and G. Agarwal, Phys. Rev. A **50**, 2870 (1994).
 - [3] A. Gilchrist, P. Deuar, and M. Reid, Phys. Rev. Lett. **80**, 3169 (1998).
 - [4] A. Gilchrist, P. Deuar, and M. Reid, Phys. Rev. A. **60**, 4259 (1999).
 - [5] E. Schrödinger, Naturwissenschaften **23**, 844 (1935).
 - [6] W. Munro, Phys. Rev. A **59**, 4197 (1999).
 - [7] J. Clauser and M. Horne, Phys. Rev. D **10**, 526 (1974).
 - [8] V. Buzek, A. Vidiella-Barranco, and P. L. Knight, Phys. Rev. A **45**, 6570 (1992).
 - [9] G. Agarwal, Phys. Rev. Lett. **57**, 827 (1986).
 - [10] G. Agarwal, J. Opt. Soc. Am. **5**, 1940 (1988).
 - [11] C. Gardiner and A. Parkins, Phys. Rev. A **50**, 1792 (1994).